

# Dual-Isotope Brain SPECT Imaging with Technetium-99m and Iodine-123: Clinical Validation Using Xenon-133 SPECT

Michael D. Devous, Sr., J. Kelly Payne and James L. Lowe

*Nuclear Medicine Center and Department of Radiology, The University of Texas Southwestern Medical Center, Dallas, Texas*

**Editor's Note:** See also "Dual-Isotope Brain SPECT Imaging with Technetium-99m and Iodine-123: Validation by Phantom Studies" on page 2030

Our phantom studies indicate that the energy resolution (9.7% FWHM) of a new three-headed single-photon tomograph (PRISM-3000) separates the distribution of  $^{99m}\text{Tc}$  from  $^{123}\text{I}$  for 10% asymmetric or 15% or 10% centered  $^{99m}\text{Tc}$  windows when combined with a 10% asymmetric  $^{123}\text{I}$  window. This technique is now applied to the simultaneous measurement of resting rCBF and changes induced by vasodilation (1 g acetazolamide) in 10 subjects with cerebrovascular disease. Resting and vasodilated  $^{133}\text{Xe}$  SPECT images were obtained first. Within 48 hr,  $^{99m}\text{Tc}$  HMPAO was given at rest, acetazolamide injected, and after 20 min either [ $^{123}\text{I}$ ] IMP or [ $^{123}\text{I}$ ] HIPDM was administered. Subjects were scanned for  $^{99m}\text{Tc}$  and  $^{123}\text{I}$  simultaneously using 10% asymmetric windows. Regression analyses demonstrated a linear relationship between  $^{133}\text{Xe}$  SPECT and dual-isotope SPECT measurements of lesion-to-cerebellum ratios in baseline ( $r = 0.92$ ), vasodilated ( $r = 0.86$ ) and rest-minus-vasodilated data ( $r = 0.85$ ). Technetium-99m and  $^{123}\text{I}$  images obtained through dual-isotope imaging are by definition in perfect anatomic registration.

**J Nucl Med 1992; 33:1919-1924**

Measurements of regional cerebral blood flow (rCBF) by single-photon emission computed tomography (SPECT) have been used extensively in patients with cerebrovascular disease (1-3). rCBF SPECT may provide the earliest imaging evidence of cerebral ischemia in acute stroke patients. Further, rCBF images may provide the best documentation of the status of the cerebrovascular system in at-risk patients, such as those suffering from transient ischemic attacks (TIAs) (2,4). The primary information provided by conventional SPECT techniques is

the distribution of diminished perfusion or hyperemia seen in the resting state. These data can be used to assess the degree to which observed structural lesions (CT or MRI) properly represent the affected territories and to assess the severity of purely functional alterations. Recently, several studies have also suggested that resting rCBF imaging might provide a prognostic indicator of recovery from either motor or language deficits (5-10).

Unfortunately, such measurements do not address the important issue of diminished vasodilatory reserve. The vascular system of the brain is controlled by autoregulatory processes. When these are disturbed by atherosclerosis, thrombi or vasospasm, the ability of the cerebrovascular system to compensate is compromised. When compensation does occur, resting rCBF may appear normal or minimally altered. It is therefore important to determine the degree to which underlying disease has exhausted the normal reserve capacity and the degree to which collateral supplies have been recruited as a countermeasure.

Our group (11,12) and several others (2,13-15) have worked to develop a "brain stress test" that will reflect vasodilatory reserve. Carbon dioxide is an effective vasodilator in the cerebrovascular system. A convenient and effective alternative is the administration of acetazolamide (Diamox, Lederle), a carbonic anhydrase inhibitor. Intravenous administration of 1 g acetazolamide leads to a uniform increase in rCBF throughout the normal brain that peaks at 20 min and lasts for about 1 hr, gradually returning to normal over a 2-3-hr span. Diseased or at-risk areas show little or no response. Side effects are minimal, including mild paresthesias and diuresis.

Acetazolamide stress testing has been used to assess cerebrovascular reserve in patients with TIA, stroke, arteriovenous malformation, epilepsy and dementia (2,11-17). In the latter two instances, the purpose of the test is to determine whether alterations in resting rCBF are of neuronal or vascular origin. Primary neuronal dysfunction produces rCBF abnormalities through autoregulation and is associated with a normal acetazolamide response.

Received Dec. 16, 1991; revision accepted Jul. 1, 1992.  
For reprints contact: Dr. Michael D. Devous Sr., Nuclear Medicine Center, UT Southwestern Medical Center, 5323 Harry Hines Blvd., Dallas, TX 75235-9061.

rCBF imaging of cerebrovascular reserve requires comparison of resting rCBF images to those obtained 20–30 min after acetazolamide injection. Most of the work done to illustrate the usefulness of this technique has employed SPECT rCBF imaging with  $^{133}\text{Xe}$ . Since  $^{133}\text{Xe}$  rapidly clears from the body, acetazolamide-activated rCBF images can be obtained shortly after the resting images. Unfortunately,  $^{133}\text{Xe}$  SPECT is not yet widely available. More readily available agents for rCBF SPECT have prolonged brain retention times. With these agents (or  $^{18}\text{F}$ FDG PET), it is not possible to study two brain conditions within a short time period. As a result, conventional SPECT measurements of cerebrovascular reserve must be made on two occasions, typically separated by 24–48 hr. In contrast,  $^{133}\text{Xe}$  SPECT and  $^{15}\text{O}$  or  $^{11}\text{C}$  PET measurements can be repeated in a single sitting in an individual subject.

Nevertheless, it might be possible to use SPECT brain imaging agents labeled with two different radioisotopes ( $^{99\text{m}}\text{Tc}$  and  $^{123}\text{I}$ ) to sequentially examine resting and vasodilated rCBF. For many years, nuclear medicine gamma cameras have had the capacity to record from multiple photopeaks. Multiple windows have been used to correct for scatter contributions by recording from both photopeak and Compton scatter windows (18,19). Sequential and simultaneous imaging of  $^{201}\text{Tl}$  and  $^{99\text{m}}\text{Tc}$  has been employed in cardiac studies (20–25). However, typical gamma camera energy resolution (12%–15% FWHM) provides insufficient resolving power to separate 140 keV ( $^{99\text{m}}\text{Tc}$ ) from 160 keV ( $^{123}\text{I}$ ) photopeaks. Fortunately, the demands of high-resolution multi-detector SPECT have required enhanced performance characteristics, including substantially improved energy resolution. The tomograph used in these studies (PRISM-3000, Picker, Cleveland, OH) has an energy resolution of 9.7% FWHM, 20.0% FWTM, which might be adequate to resolve  $^{99\text{m}}\text{Tc}$  and  $^{123}\text{I}$ .

Even at this resolution there is substantial photopeak overlap. By using phantoms, we examined the effect of this overlap on isotope discrimination as a function of window width and position and on quantitative count recovery (26). We now report the results of a clinical investigation of the simultaneous measurement of resting rCBF with  $^{99\text{m}}\text{Tc}$ -HMPAO and acetazolamide-vasodilated rCBF with [ $^{123}\text{I}$ ]JIMP or HIPDM as a test of vasodilatory reserve. We compared dual-isotope results to those obtained using sequential  $^{133}\text{Xe}$  SPECT scans (pre- and post-acetazolamide) in subjects with known stable cerebrovascular disease.

## METHODS

Ten subjects with stable cerebrovascular disease were studied with  $^{133}\text{Xe}$  SPECT and with the dual-isotope technique before and after cerebral vasodilation with acetazolamide. The imaging protocol is as described below. There were three females and seven males ranging in age from 43 to 63 yr. Six subjects previ-

ously had strokes, and four suffered from TIA. CT demonstrated unilateral cortical and subcortical infarcts in 7/10 subjects. Three TIA patients had normal CT. All subjects were imaged at least 30 days after their most recent ictus and had no change in neurologic status over the course of these experiments. All subjects gave informed consent as approved by the Institutional Review Board of the University of Texas Southwestern Medical Center.

## Scanning Procedures

On Day 1, subjects underwent a resting  $^{133}\text{Xe}$  SPECT study, then received 1 g acetazolamide intravenously. After a 20-min delay, a vasodilated  $^{133}\text{Xe}$  SPECT image set was obtained. rCBF was measured by  $^{133}\text{Xe}$  SPECT in three tomographic cross-sections with centers 4 cm apart using the Tomomatic 64 (Medimatic A/S, Copenhagen, Denmark). Xenon-133 was administered in an air/oxygen mixture (10 mCi/liter) by inhalation during the first minute of a 4-min washin/washout procedure. The subjects breathed room air during the remaining three minutes of the study. Subjects were positioned in the tomograph using a face-marking template so that cross sections were obtained 2, 6 and 10 cm above and parallel to the cantho-meatal line (CML). They were studied in a dimly lit environment, with eyes and ears open. Background noise consisted only of machine cooling fans. These procedures and values in normal subjects, reproducibility, intersubject variability and asymmetries have been described in detail by Devous et al. (27).

On Day 2, subjects received 20 mCi  $^{99\text{m}}\text{Tc}$ -HMPAO intravenously, then, after a 10-min delay, 1 g acetazolamide. Following another 20 min delay subjects received either 3–5 mCi [ $^{123}\text{I}$ ]JIMP or 10–12 mCi [ $^{123}\text{I}$ ]HIPDM. After a final 20-min delay, dual-isotope SPECT images were obtained using 10% wide asymmetric windows to separate the distribution of  $^{99\text{m}}\text{Tc}$  (using the lower half of the photopeak) from  $^{123}\text{I}$  (using the upper half of the photopeak). We chose  $^{99\text{m}}\text{Tc}$ -HMPAO for resting studies and  $^{123}\text{I}$ -labeled agents for vasodilated studies because there is preliminary evidence that the iodinated agents follow high-flow states more accurately than  $^{99\text{m}}\text{Tc}$ -HMPAO.

Technetium-99m and  $^{123}\text{I}$  images were obtained with subjects in the supine position and aligned by visual inspection with their CML perpendicular to the axis of rotation. As with  $^{133}\text{Xe}$  SPECT, subjects were injected with eyes and ears open, in a dimly lit environment with machine cooling fans providing the only background noise. High-resolution fan-beam collimators were placed at a radius of 13 cm from the center of rotation. Projection data were acquired in a  $128 \times 128$  matrix in 3-degree angular increments over a total study time of 40 min. This study duration is approximately twice that normally used with single-isotope studies to compensate for the reduced counting efficiency of asymmetric windows.

## Image Reconstruction

For  $^{133}\text{Xe}$  SPECT, three tomographic cross sections were generated by filtered backprojection and attenuation corrected. rCBF was calculated according to the double-integral method (2,3,27). rCBF images were displayed in a  $64 \times 64$  matrix employing a 16-shade scale adjusted to range from zero flow to maximum flow. Transverse resolution is 1.7 cm and axial resolution is 1.9 cm.

For high-resolution SPECT, projection data were prefiltered using a low-pass Butterworth filter adjusted for each subject, but with an order in the range of 8 to 10 and with a cutoff frequency

ranging from 0.2 to 0.3 cycles/pixel. Images were reconstructed in the transverse domain using backprojection with a third-order Butterworth filter at a cutoff frequency of 0.2 to 0.3 cycles/pixel. This resulted in 1.9 mm thick slices which were attenuation corrected using a first-order method. Subsequently, coronal and sagittal images were obtained from the transverse set and all image sets were summed to a final slice thickness of 5.8 mm. In-plane resolution varied from approximately 6 mm at the cortical surface to about 8 mm at the center of rotation. Surface-rendered three-dimensional images were produced for display purposes using a threshold setting of approximately 80% of the mean cortical gray matter count density in normal regions.

### Data Analysis

Areas of reduced perfusion in resting  $^{133}\text{Xe}$  images were identified by visual inspection and the entire lesion was outlined to form the "abnormal" region of interest (ROI). Only one region per subject was examined. A ROI was also placed in the ipsilateral cerebellum to serve as a "normal" area since no subject had CT evidence of bilateral disease. These regions were saved on disk and reproduced by an automated fitting routine in the vasodilated images (post-acetazolamide). The ROI defined in the resting image was not modified for the vasodilated study if a larger "lesion" was observed after acetazolamide. If no abnormalities were observed at rest ( $n = 2$ ), then areas of *relative* hypoperfusion seen after acetazolamide were used to circumscribe "at-risk" ROIs. At-risk ROIs were then reproduced in the same location in the corresponding resting studies as described above. Ipsilateral cerebellar ROIs were again used to represent normal zones. An abnormal-to-cerebellum or at-risk-to-cerebellum flow ratio was computed for both resting and vasodilated studies for each subject. Finally, the change in a regional flow ratio between resting and vasodilated states was computed by subtracting vasodilated flow ratios from baseline flow ratios.

ROI placement in the dual-isotope studies approximately replicated that determined by the  $^{133}\text{Xe}$  images. The image resolution of the two techniques is not comparable. However, atlas guidelines (28) indicate that the slice 6 cm above the CML is centered just above the thalamic nuclei. Therefore, dual-isotope ROIs were placed in the first slice above the thalamic nuclei. These were hand drawn to match images of  $^{133}\text{Xe}$  ROIs rather than to conform to characteristics of the dual-isotope images themselves. We recognize that this approach does not yield perfect replication of ROI placement between the two data sets. Unfortunately, the physical design of the Tomomatic 64 precludes the use of external markers (radioactive sources or restraint masks) that could be used for more precise comparisons. Our approach might limit, but should not enhance, the likelihood of observing a significant relationship between the two modalities. An ipsilateral cerebellar ROI was placed in a transverse slice demonstrating clear separation of cerebellum from surrounding cortical tissues. As above, lesion-to-cerebellum flow ratios were computed for both resting and vasodilated studies for all subjects. Again, the change in a regional flow ratio between resting and vasodilated states was computed by subtracting vasodilated flow ratios from baseline flow ratios.

Baseline, vasodilated and change data (mean ROI values) for each subject were entered into linear regression analyses to examine potential relations between  $^{133}\text{Xe}$  SPECT and dual-isotope SPECT. Regression coefficients, slopes and intercepts were calculated.

## RESULTS

A typical example of failed vasodilator reserve measured by  $^{133}\text{Xe}$  SPECT is shown in Figure 1. Subject GW demonstrates mild left hemispheric hypoperfusion in the resting images and severe vasodilatory reserve failure in the same territory after acetazolamide (Diamox). Technetium-99m-HMPAO resting images (top, Fig. 2) replicate the mild left hemispheric hypoperfusion seen in the baseline  $^{133}\text{Xe}$  images. Similarly, the post-Diamox [ $^{123}\text{I}$ ]IMP images (bottom, Fig. 2) clearly illustrate the distribution of failed vasodilatory reserve. A three-dimensional surface rendered demonstration of these data is shown in Figure 3.

In all subjects, the changes induced by vasodilation observed with  $^{133}\text{Xe}$  were also seen in dual-isotope images. The lesion volumes were not quantitatively compared since the profound differences in spatial resolution preclude a useful analysis. However, as expected, lesion definition was clearer in the high resolution studies. In some subjects, abnormalities not noted by  $^{133}\text{Xe}$  due to limited slice sampling were clearly evidenced by the full-volume imaging technique.

Baseline regression results are shown at the top of Figure 4. A strong linear correlation ( $r = 0.92$ ) was observed. The slope ( $0.89 \pm 0.13$ ,  $\pm$  s.e.) was not significantly different from one and the intercept ( $0.09 \pm 0.11$ ) was not significantly different from zero. Absolute flow values at rest in lesion ROIs using  $^{133}\text{Xe}$  SPECT ranged from 35 to 62 ml/min/100 g, while baseline cerebellar flows ranged from 43 to 71 ml/min/100 g.

Vasodilated image regression results are shown in the middle of Figure 4. Again a linear relationship was observed ( $r = 0.86$ ) without significant changes in slope ( $0.92 \pm 0.19$ ) or intercept ( $0.00 \pm 0.15$ ) from those observed in the baseline state. However, the data were more variable, as reflected in the slightly poorer fit and larger standard errors. Absolute flow values in lesion ROIs following vasodilation using  $^{133}\text{Xe}$  SPECT ranged from 47 to 82 ml/min/100 g, while cerebellar flows ranged from 67 to 107 ml/min/100 g. There was a 38% mean increase in cerebellar flow after acetazolamide.

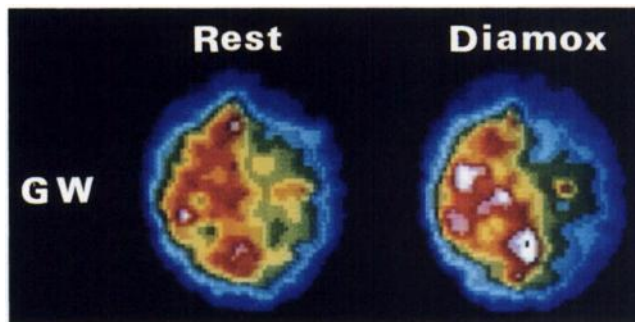


**FIGURE 1.** Xenon-133 rCBF images (6 cm above and parallel to the cantho-meatal line) in subject with both resting flow abnormalities and loss of vasodilatory reserve (seen following acetazolamine [Diamox]-induced vasodilation). Subject GW was imaged after a TIA.

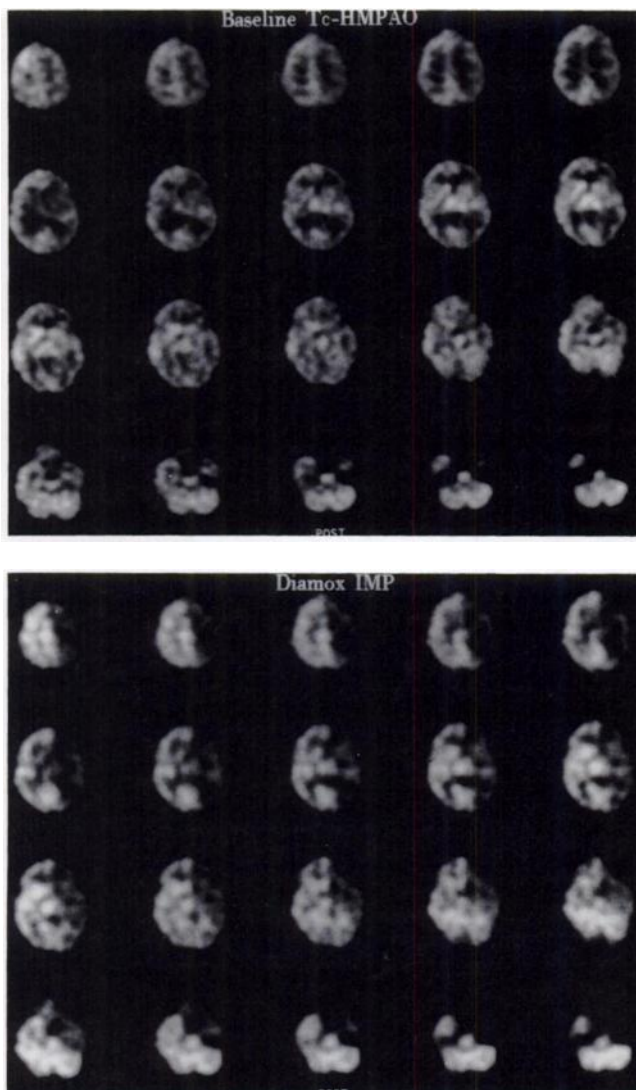


**FIGURE 2.** Dual-isotope images from Subject GW showing mild left-hemispheric hypoperfusion at rest (top,  $^{99m}\text{Tc}$ -HMPAO) and an enlarged at-risk area of failed vasodilatory reserve following Diamox (bottom, [ $^{123}\text{I}$ ]IMP).

Similarly, the change in flow ratios induced by vasodilation was linearly related ( $r = 0.85$ ) between the two approaches (bottom, Fig. 4). Once again the slope ( $0.87 \pm 0.19$ ) did not differ from one and the intercept ( $0.06 \pm 0.02$ ) did not differ from zero. Nine of ten subjects had values greater than zero. Thus, flow ratios after vasodilation were lower than at baseline, consistent with some degree of reserve failure.

#### DISCUSSION

Phantom studies using this tomograph (26) concluded that: (1) energy resolution below 10% is adequate to permit separation of  $^{99m}\text{Tc}$  and  $^{123}\text{I}$  using 10% asymmetric windows; (2) 10% asymmetric windows produce images that are  $\approx 95\%$  derived from the isotope of interest for a 4/1 Tc/I concentration ratio; and (3) quantitative recovery of count distributions is not significantly altered by dual-

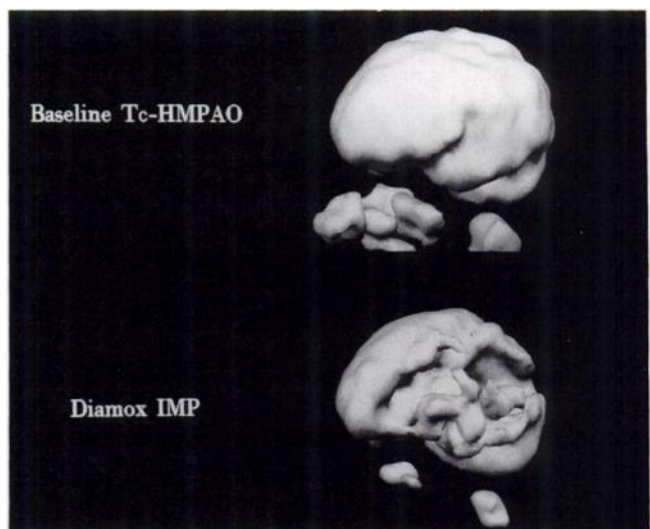


**FIGURE 3.** Three-dimensional displays of resting (top) and vasodilated (bottom) rCBF in Subject GW. These surface-rendered images were created with identical thresholds for technetium and iodine, chosen to maintain a continuous surface in the resting images. This procedure highlights the distribution of failed vasodilatory reserve.

isotope acquisitions. In this study, we compared resting and vasodilated  $^{133}\text{Xe}$  SPECT images to resting ( $^{99m}\text{Tc}$ -HMPAO) and vasodilated ([ $^{123}\text{I}$ ]IMP or HIPDM) dual-isotope images in ten patients with cerebrovascular disease.

Visual inspection of image pairs indicated that vasodi-

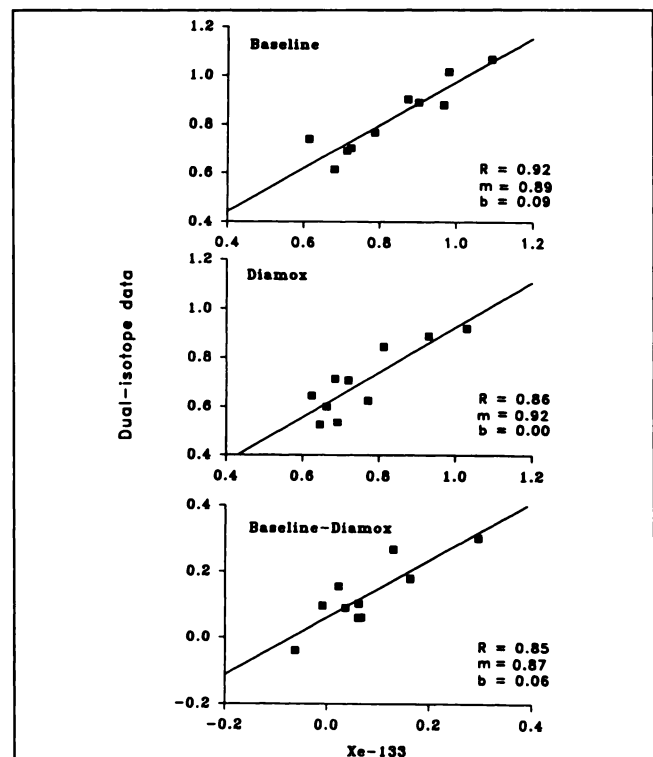


**FIGURE 4.** Regression analysis of lesion-to-cerebellum ratios from baseline (top), vasodilated (Diamox, middle) and rest-minus-vasodilated (bottom)  $^{133}\text{Xe}$  and  $^{99m}\text{Tc}$  images. R = regression coefficient; m = slope; b = intercept.

latory reserve measurements by dual-isotope imaging of HMPAO (resting rCBF) and IMP or HIPDM (post-acetazolamide rCBF) parallel results obtained with sequential  $^{133}\text{Xe}$  SPECT scans. Regression analyses comparing  $^{133}\text{Xe}$  and dual-isotope studies demonstrated linear correlations for baseline, vasodilated and rest-vasodilated data. There was clearly somewhat greater scatter in the clinical data than in the phantom studies. This is not surprising given the strikingly different spatial resolutions of the two imaging systems. ROI placement might also contribute to data scatter since slice alignment between tomographs was done by visual inspection rather than by a formal subject registration system. Consequently, these data likely provide a conservative measure of the degree of agreement between the two methods of vasodilatory reserve measurement.

It is interesting that the slopes for the baseline and vasodilated sets did not differ from one and that the intercepts did not differ from zero. This implies, at least for data normalized to cerebellum, that  $^{99\text{m}}\text{Tc}$ -HMPAO follows rCBF linearly up to 60 ml/min/100 g. Similarly, our data suggest that normalized data from the iodinated amines are linearly related to rCBF up to 82 ml/min/100 g.

Finally, a significant secondary benefit of dual-isotope imaging is that the  $^{99\text{m}}\text{Tc}$  and  $^{123}\text{I}$  images are by definition in perfect anatomic registration. This facilitates quantitative assessments of the degree and location of vasodilatory reserve failure. An illustration of subtraction imaging to identify the tissues experiencing reserve failure is provided in Figure 5. These images are also from Subject GW (see Figs. 1–3). A 20% background was subtracted from the  $^{99\text{m}}\text{Tc}$ -HMPAO data to correct for nonbrain tissue background and scatter and a 10% scatter background was removed from the  $^{123}\text{I}$ IMP data (only for the purposes of this illustration). Subsequently, paired cerebellar ROIs were used to determine a scaling factor in order to nor-

malize the data sets. Normalized  $^{123}\text{I}$ IMP images (middle row) were then slice-by-slice subtracted from  $^{99\text{m}}\text{Tc}$ -HMPAO images (top row). Residual activity is taken to represent areas of failed reserve (bottom row).

In summary, this technique permits simultaneous imaging of  $^{99\text{m}}\text{Tc}$ - and  $^{123}\text{I}$ -labeled brain radiopharmaceuticals administered to a single subject. The current study documents the effectiveness of this technique in monitoring vasodilatory reserve. Furthermore, one can monitor any circumstance potentially producing a change in the perfusion state within 24 hr due to the in vivo stability of  $^{99\text{m}}\text{Tc}$ -HMPAO. Additional applications for dual-isotope imaging include ictal/interictal seizure imaging, monitoring acute therapeutic interventions and single-session evaluations of cognitive or pharmaceutical challenge tests. Similarly, it would be possible to use this technique in receptor modeling studies by directly measuring rCBF (normally deduced by assumption) with a  $^{99\text{m}}\text{Tc}$ -labeled flow tracer, while simultaneously using an  $^{123}\text{I}$ -labeled receptor ligand.

#### ACKNOWLEDGMENTS

The authors wish to express their appreciation for the expert technical assistance of S.K. Gassaway and the engineering support provided by F. Valentino (Ohio Imaging/Picker). The many useful discussions with and advice of Dr. Jonathan Links were invaluable.

#### REFERENCES

1. Helman RS, Tikofsky RS. An overview of the contribution of regional cerebral blood flow studies in cerebrovascular disease. *Semin Nucl Med* 1990;20:303–324.
2. Vorstrup S. Tomographic cerebral blood flow measurements in patients with ischemic cerebrovascular disease and evaluation of the vasodilatory capacity by the acetazolamide test. *Acta Neurol Scand* 1988;77(suppl 114):5–47.
3. Devous MD Sr, Stokely EM, Bonte FJ. Quantitative imaging of regional cerebral blood flow in man by dynamic single-photon tomography. In: Homan BL, ed. *Radionuclide imaging of the brain*. New York: Churchill Livingstone; 1985:135–162.
4. Vorstrup S, Hemmingsen R, Henriksen L, et al. Regional cerebral blood flow in patients with transient ischemic attacks studied by Xe-133 inhalation and emission tomography. *Stroke* 1983;14:903–910.
5. Mountz JM, Modell JG, Foster NL, et al. Prognostication of recovery following stroke using the comparison of CT and Tc-99m HM-PAO SPECT. *J Nucl Med* 1990;31:61–66.
6. Limburg M, van Royen EA, Hijdra A, Verbeeten B Jr. rCBF-SPECT in brain infarction: when does it predict outcome? *J Nucl Med* 1991;32:382–387.
7. Vallar G, Perani D, Cappa SF, Messa C, Lenzi GL, Fazio F. Recovery from aphasia and neglect after subcortical stroke: neuropsychological and cerebral perfusion study. *J Neurol Neurosurg Psych* 1988;51:1269–1276.
8. Giubilei F, Lenzi GL, Di Piero V, et al. Predictive value of brain perfusion single-photon emission computed tomography in acute ischemic stroke. *Stroke* 1990;21:895–900.
9. Bushnell DL, Gupta S, Micoch AG, Barnes WE. Prediction of language and neurologic recovery after cerebral infarction with SPECT imaging using N-isopropyl-p-(I-123)iodoamphetamine. *Arch Neurol* 1989;46:665–669.
10. Hayman LA, Taber KH, Jhingran SG, et al. Cerebral infarction: diagnosis and assessment of prognosis by using  $^{123}\text{I}$ IMP-SPECT and CT. *AJNR* 1989;10:557–562.
11. Bonte FJ, Devous MD Sr, Reisch JS. The effect of acetazolamide on regional blood flow in normal human subjects as measured by single-photon emission computed tomography. *Invest Radiol* 1988;23:564–568.
12. Bonte FJ, Devous MD Sr, Reisch JS, et al. The effect of acetazolamide on

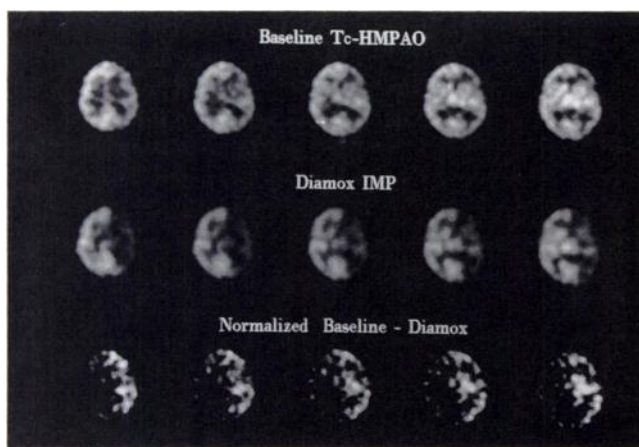


**FIGURE 5.** Baseline (top) and count-normalized vasodilated (middle) images from Subject GW. Inherent image registration properties of dual-isotope imaging permit direct slice-by-slice subtraction (bottom) once scaling adjustments for differences in count densities have been made.

- regional cerebral blood flow in patients with Alzheimer's disease or stroke as measured by single-photon emission computed tomography. *Invest Radiol* 1989;24:99-103.
13. Vorstrup S, Brun B, Lassen NA. Evaluation of the cerebral vasodilatory capacity by the acetazolamide test before EC-IC bypass surgery in patients with occlusion of the internal carotid artery. *Stroke* 1986;17:1291-1298.
  14. Chollet F, Celsis P, Clanet M, et al. SPECT study of cerebral blood flow reactivity after acetazolamide in patients with transient ischemic attacks. *Stroke* 1989;20:458-464.
  15. Højer-Pedersen E. Effect of acetazolamide on cerebral blood flow in subacute and chronic cerebrovascular disease. *Stroke* 1987;18:887-891.
  16. Devous MD Sr, Batjer HH, Mickey B, et al. Dynamic SPECT measurements of vasodilatory reserve in regions of cerebral steal in patients with arteriovenous malformations. *J Cereb Blood Flow Metab* 1987;7:S200-201.
  17. Devous MD Sr, Homan RW, Bonte FJ. Cerebral vascular reactivity in patients with partial complex epilepsy. *J Nucl Med* 1987;28:408.
  18. Koral KF, Swailem FM, Buchbinder S, Clinthorne NH, Rogers WL, Choi BMW. SPECT dual-energy window Compton correction: scatter multiplier required for quantification. *J Nucl Med* 1990;31:90-98.
  19. Jaszczak RJ, Greer KL, Floyd CE, Harris CC, Coleman RE. Improved SPECT quantification using compensation of scattered photons. *J Nucl Med* 1984;25:893-900.
  20. Fujii T, Kanai H, Mirayama J, et al. Myocardial imaging with thallium-201—subtraction imaging with  $^{201}\text{TlCl}$  and  $^{99\text{m}}\text{TcO}_4^-$  for the visualization of the right ventricle. *Radioisotopes* 1979;28:751-756.
  21. Johnson LL, Seldin DW. The role of antimyosin antibodies in acute myocardial infarction. *Semin Nucl Med* 1989;19:238-246.
  22. Johnson LL, Seldin DW, Keller AM, et al. Dual isotope thallium and indium antimyosin SPECT imaging to identify acute infarct patients at further ischemic risk. *Circulation* 1990;81:37-45.
  23. Kitahara K, Suzuki S, Takayama Y, Hiroe M. New color imaging of [ $^{99\text{m}}\text{Tc}$ ]-pyrophosphate and [ $^{201}\text{Tl}$ ]-chloride dual isotope single photon emission computed tomography in acute myocarditis. *Jpn J Nucl Med* 1989;26:773-779.
  24. Kawaguchi K, Sone T, Tsuboi H, et al. Quantitative estimation of infarct size by simultaneous dual radionuclide single photon emission computed tomography: comparison with peak serum creatine kinase activity. *Am Heart J* 1991;121:1353-1360.
  25. Nishimura T, Uehara T, Oka H, et al. Serial assessment of denervated but viable myocardium following acute myocardial infarction by using  $^{123}\text{I}$ -MIBG and  $^{201}\text{TlCl}$  myocardial SPECT. *Jpn J Nucl Med* 1990;27:709-718.
  26. Devous MD Sr, Lowe JL, Payne JK. Dual-isotope brain SPECT imaging with  $^{99\text{m}}\text{Tc}$  and  $^{123}\text{I}$ : validation by phantom studies. *J Nucl Med* 1992;33:2030-2035.
  27. Devous MD Sr, Bonte FJ, Stokely EM. The normal distribution of regional cerebral blood flow measured by dynamic single-photon emission tomography. *J Cereb Blood Flow Metab* 1986;6:95-104.
  28. Matsui T, Hirano A. *An atlas of the human brain for computerized tomography*. Tokyo, New York: Agaku-Shoin, 1978:147-151.